Analysis Method of Pyrolysis Kinetics Using Modern Signal Processing Techniques

Truls Liliedahl, Krister Sjöström, and Lars-Peter Wiktorsson
Institutionen för Kemisk Teknologi, Kungl Tekniska Högskolan, S-100 44 Stockholm, Sweden

Coal pyrolysis kinetics has been discussed for many years in numerous articles and reports. They include the following studies: Anthony et al. (1974), Badzioch and Hawksley (1970), Eklund et al. (1987), Jüntgen and van Heek (1970), Jüntgen (1984), Kobayashi et al. (1977), Seehra and Ghosh (1988), Solomon et al. (1982), Solomon and Hamblen (1983), Solomon et al. (1986), and Suuberg et al. (1978). Nevertheless, uncertainties still exist. Activation energies and frequency factors, for example, tend to be so specific that they sometimes can be looked upon rather as experimental correlation parameters, not as factors reflecting chemical properties. One reason for this may be the uncertainty and diversity of methods used, apart from the complexity of pyrolysis reactions (Solomon and Hamblen, 1983; Solomon et al., 1986).

The practical as well as theoretical aspects of pyrolysis in an environment of nonconstant temperature (that is, nonisothermal pyrolysis) have been discussed extensively by Jüntgen and van Heek (1970) and Jüntgen (1984) among others. Nonisothermal methods are preferable if experiments are to be evaluated in the context of applied process conditions that imply slow heating rates. A drawback with the nonisothermal approach is the complicated kinetic expression. If applied process conditions imply fast heating rates, however, pyrolysis experiments in a constant temperature environment (that is, isothermal pyrolysis) is preferable. Isothermal methods also result in less complicated kinetic expressions.

This study is aimed at developing a coherent method for deriving true devolatilization over time while coal, peat or biomass is pyrolyzed in a constant-temperature environment. The analysis of instantaneous reaction rates over time under isothermal conditions could open up the possibility of correlating the simpler single-reaction model to the more complicated, but more correct, multiple-reaction models, such as the one suggested by Anthony et al. (1974). The devolatilization profile will also allow for the analysis of the initial heat-transfer-limited devolatilization. The quality of modeling of pyrolysis applications also may be enhanced, if kinetic parameters are derived at conditions similar to process applications.

The experimental setup consisted of a gas chromatograph (GC) equipped with a pyrolysis unit, an empty column, and a detector. The method uses the mathematical principle that the observed detector response equals the convolution of the true devolatilization and the residence time distribution (RTD). Using Fourier transformation and filter algorithms, it was possible to derive or deconvolve the true devolatilization from the observed one and the RTD.

Experimental Setup

The experimental apparatus consisted of a GC equipped with a Pyrojector (from Scientific Glass Engineering, Ltd., Ringwood, Victoria, 3134 Australia) as injector, an empty column, and a flame ionization detector (FID) in series (Figure 1). The column was empty, as its sole purpose was to transfer the entrained volatiles from the Pyrojector to the detector. Detector signals were sampled on-line on a desk-top computer using an A/D converter. For data handling, the MatLab software with the auxiliary Signal Processing Toolbox (from The MathWorks, Inc., South Natick, MA) was used.

Theory

The detector response $f(t)$ of an instantaneously injected tracer at given experimental conditions is defined as:

$$a = \int_0^\infty f(t)dt \tag{1}$$

If the instantaneous tracer injection simulates the Dirac delta function, the residence time distribution will be given by:

$$\text{RTD} = \frac{f(t)}{a} \tag{2}$$

For the devolatilization of an instantaneously injected solids sample, the following assumption is made:

$$g(t) = \frac{dV_t}{dt} = H(t) \cdot k \cdot (V_\infty - V_t)^n \tag{3}$$

Correspondence concerning this work should be addressed to T. Liliedahl.

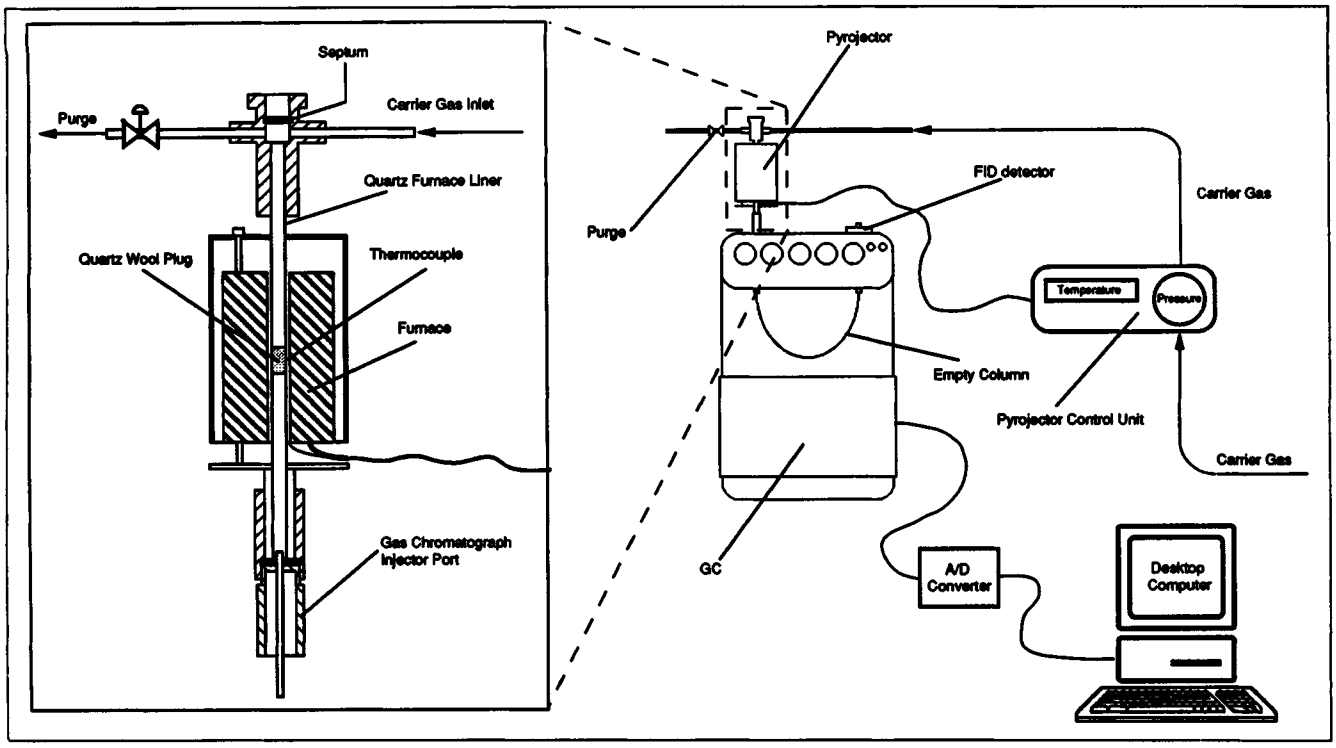

Figure 1. Experimental set-up and pyrojector (enlarged).

with the reaction rate constant k given by the Arrhenius expression:

$$k = k_0 \cdot e - \frac{E}{RT} \tag{4}$$

Equation 3 can be rewritten and re-arranged, if the amounts of volatile matter are normalized relative to the tracer amount following $g'(t) = [g(t)]/a$; $V'_\infty = V_\infty/a$; and $V'_t = V_t/a$:

$$g'(t) = H(t) \cdot k \cdot a^{n-1} \cdot {V'_\infty}^n \cdot \left(1 - \frac{V'_t}{V'_\infty}\right)^n \tag{5}$$

The true normalized devolatilization $g'(t)$ will be overlaid by the RTD, resulting in the observed normalized detector response $h'(t)$. Thus, $h'(t)$ is given by the convolution integral (Levenspiel, 1972):

$$h'(t) = \int_0^\infty g'(t-x)\mathrm{RTD}\,dx \tag{6}$$

Equation 6 having convolution denoted with * becomes:

$$h'(t) = g'(t) * \mathrm{RTD} \tag{7}$$

As convolution in the time plane equals multiplication in the frequency plane, Eq. 7 can be rewritten using Fourier transforms:

$$F[h'(t)] = F[g'(t)] \cdot F[\mathrm{RTD}] \tag{8}$$

Finally, its re-arrangement and inverse Fourier transformation give the normalized true devolatilization:

$$g'(t) = F^{-1}\left[\frac{F[h'(t)]}{F[\mathrm{RTD}]}\right] \tag{9}$$

In contrast to convolution, deconvolution is very sensitive to noise in the transfer function (RTD). Deconvolution following Eq. 9 will, therefore, render nonsense, and thus $g'(t)$ must be filtered.

Experimental Procedure

For determining the devolatilization profile to be deconvolved, about 1 mg of, for example, coal is instantaneously injected into the pyrojector with a solids injector or syringe. After injection, the sample will rest on the quartz wool plug inside the quartz tube of the pyrojector (Figure 1). Volatiles leaving the sample are entrained by the carrier gas through the column into the detector.

For determining the apparatus RTD, the Dirac delta function is simulated by injecting with a gas syringe instantaneously, at the height of the quartz wool plug, 0.5-1.0 mL of gaseous hydrocarbon tracer into the pyrojector. The syringe is equipped with a spring for enhancing reproducibility and ensuring an almost instantaneous injection.

In the Pyrojector, heat transfer into the particle will be mainly through convection from the gas bulk and, at high temperatures, through radiation. Thus, heat transfer is not through contact with metal surfaces, as is the case for some of the alternative pyrolysis units. This is advantageous, since heat transfer into and within the particle will be relatively homogeneous and shows similarities with conditions in pyr-

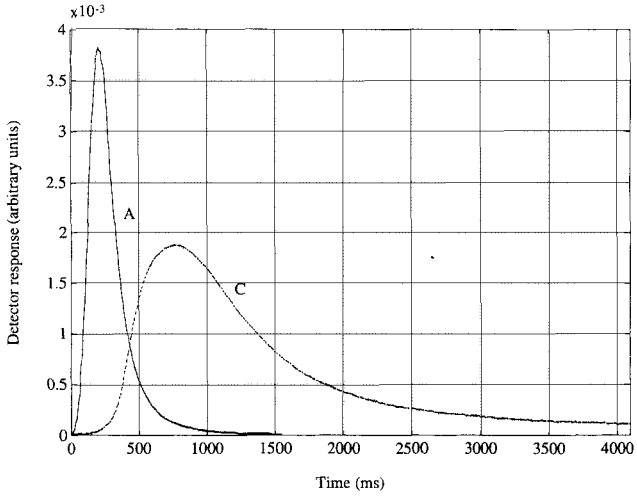

Figure 2. Files *A* and *C* after zero-time adjustment and normalization.

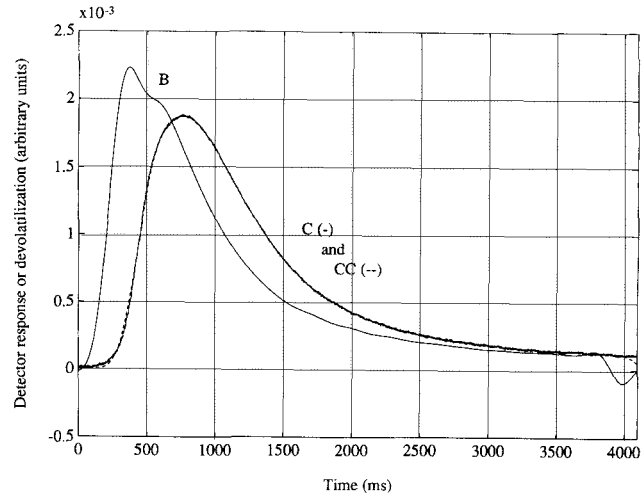

Figure 3. File *B* after filtering and files *C* and *CC*.

olysis application. For an estimate, the particle temperature can be assumed to equal that of the Pyrojector (that is, the pyrojector wall temperature). For more accurate temperature estimates, the heat transfer equations of, for example, Nilsson (1990) or Solomon et al. (1986) can be used.

The FID signals are digitalized in an A/D converter and sampled on an IBM-compatible PC. Normally, 4,096 values are stored at 1,000 Hz. Files are re-arranged and compiled into text or ASCII format for further handling.

Data Handling and Programming

The tracer injection and the pyrolysis detector responses are stored in MatLab as vectors A and C, respectively. A program written in MatLab was used for deriving the true devolatilization B from A and C (see the Appendix). In the following, the main parts of this program will be discussed through a pyrolysis experiment, in which about 1 mg of coal was pyrolyzed at 700°C with nitrogen as the carrier gas.

Zero-time adjustment and area normalization

At first files A and C are zero time adjusted and normalized relative to the tracer amount (the sum of A). After this file A equals the RTD in agreement with Eq. 2, and file C equals $h'(t)$ as described in Eq. 7. Figure 2 shows files A and C after these re-arrangements.

Deconvolution

Equation 9 is used for deconvolving B from C and A. First, files A and C are zero-padded for preventing wraparound pollution (Press et al., 1986). Files, however, are extended further than the minimum needed for preventing the wraparound pollution. The reason for this is that if a file has to be zero-padded for any reason, it is zero-padded to the nearest power-of-two file length (512, 1,024, etc.), since the fast Fourier transformation (FFT) algorithm calls for such file lengths. File B will, after this operation, be heavily polluted and will not seem to contain any nonrandomized information.

Filtering

By analyzing the cumulative sum of B over time (the amount of volatiles having left the sample at time t), it can be concluded that B, nevertheless, contains some information. Initially, when filtering, it is the cumulative sum of B that is filtered in an iterative loop using the Butterworth filter design algorithm of the MatLab Signal Processing Toolbox (Little and Shure, 1988). The Chebyshev and elliptic filtering algorithms can also be used, but the Butterworth algorithm was chosen because it calls for the least number (two) of filter design parameters. A reason for filtering the cumulative sum is that the cumulative sum of a randomized noise, on a relative basis, cancels out over time.

In the iterative filtering, it was found preferable to differentiate the average of the cumulative sum of B before and after filtering in each loop. Filtering could also be carried out by differentiating, in a loop, the filtered cumulative sum of B directly without averaging. The advantage of the chosen approach is that the Butterworth filter design parameters will be more generally applicable, and thus less sensitive to the specific characteristics of B. A drawback with this approach is that it calls for more filtering loops, thus requiring two to three minutes longer handling time.

The Butterworth filter design parameters can be determined by a power spectrum density analysis (Kahaner et al., 1989; Little and Shure, 1988; Press et al., 1986). With the chosen approach these parameters will show a relatively wide applicability.

The repetitive numerical integration and differentiation shorten the file length by one element in each loop, thereby introducing a small error. To minimize this error and the effect of filtering startup transients, B is reversed before filtering, since errors will be introduced at the zero-padding end. After filtering, the file is flipped back again and the first 4,096 values are saved as B. The resulting file B is shown in Figure 3.

Test of correctness

The correctness of the found B is thereafter verified in accordance with Eq. 7 by convolving B with A. If the resulting vector CC approximates the original C, the quality of the

derived B is said to be good. For the discussed example, it can thus be concluded from Figure 3 that the found B approximates the true devolatilization of detectable matter over time, given that A represents the RTD. As convolution, in contrast to deconvolution, is not sensitive to noise, this operation can be carried out directly, without filtering.

For the discussed example, the total handling time is about four minutes, mainly due to the iterative filtering.

Discussion

By the analysis of the derived devolatilization profile B, the apparent or overall reaction rate constants and the reaction orders can be derived from Eqs. 3 to 5 with relative ease. By comparing experiments at different temperatures, apparent activation energies E and frequency factors k_0 can be computed.

The front side or the heat-transfer-controlled part of B can be analyzed for computing heat transfer coefficients using the heat balance expressions of Nilsson (1990), Pyle and Zaror (1984), or Solomon et al. (1986). If first-order devolatilization kinetics is assumed, this part of the profile can also be used for estimating apparent activation energies and frequency factors for this part of the profile. The activation energy is then derived in accordance with Eqs. 4 and 5, by numerical differentiation of the logarithm of the B front side. Through the estimated heat transfer coefficient, the frequency factor can then be computed. Thus, this alternative approach makes it possible to estimate activation energies and frequency factors in only one experiment.

An advantage of monitoring the instantaneous devolatilization is that the shape of the profile as such may contain valuable information. For example, the "shoulder" on the back side of profile B (Figure 3) would not have been recognized with the methods that give integral values of devolatilization. It should also be noted that this "shoulder" is not recognizable in profile C (Figure 3) to be deconvolved, due to the "smearing-out" property of the RTD.

It is possible to verify the correctness of the derived devolatilization profile B, by convolving this profile with the RTD. The correctness of the RTD, however, cannot be verified. Detector responses are also assumed to be linear with respect to the concentration of a compound, as well as between compounds. This assumption is probably fair for most detectors, such as the used FID and the thermal conductivity detector (TCD). If analyzing the devolatilization of sulfur compounds in a flame photometric detector (FPD), the nonlinearity of this detector can be compensated for as it has an approximately square-root concentration dependence.

Acknowledgment

Financial support of the National Energy Administration, Sweden, and Asea Brown Boveri (ABB Carbon) is gratefully acknowledged.

Notation

A = file, vector, or peak from detector response of instantaneously injected tracer, arbitrary units/s
a = total amount of detectable matter in tracer, arbitrary units
B = file, vector, or peak corresponding to true devolatilization of sample, arbitrary units/s
C = file, vector, or peak from detector response of sample devolatilization, arbitrary units/s
CC = file, vector, or peak being convolution of A and B, arbitrary units/s
E = (apparent) activation energy, J/mol
$f(t)$ = absolute detector response of instantaneously injected tracer, arbitrary units/s
$g(t)$ = absolute devolatilization of sample, arbitrary units/s
$g'(t)$ = same as $g(t)$, but normalized relative to tracer amount, Hz
$H(t)$ = Heaviside function, dimensionless
$h(t)$ = absolute detector response of devolatilization, arbitrary units/s
$h'(t)$ = same as $h(t)$, but normalized relative to tracer amount, Hz
k = reaction rate constant, arbitrary units^{1-n}/s
k_0 = apparent frequency factor or distribution of frequency factors, arbitrary units^{1-n}/s
n = reaction order, dimensionless
R = universal gas constant, 8.314 J/mol/K
RTD = same as $f(t)$, but normalized to tracer amount or residence time distribution, Hz
T = absolute temperature, K
t = time, s
V_t = volatile matter having left sample at time t, arbitrary units
V'_t = same as V_t, but normalized relative to tracer amount, dimensionless
V_∞ = total volatile matter in sample, arbitrary units
V'_∞ = same as V_∞, but normalized relative to tracer amount, dimensionless
x = dummy variable, s

Literature Cited

Anthony, D. B., J. B. Howard, H. C. Hottel, and H. P. Meissner, "Rapid Devolatilization of Pulverized Coal," *Int. Symp. on Combustion*, p. 1303, Combustion Institute, Pittsburgh (1974).

Badzioch, S., and P. G. Hawksley, "Kinetics of Thermal Decomposition of Pulverized Coal Particles," *Ind. Eng. Chem. Process Des. Dev.*, **9**(4), 521 (1970).

Eklund, G., J. R. Pedersen, and B. Strömberg, "Determination of Combustible Volatile Matter in Fuels," *Fuel*, **66**(1), 13 (1987).

Jüntgen, H., and K. H. van Heek, "Reaktionsabläufe unter nichtisothermen Bedingungen," *Fortschritte der Chemischen Forschung*, **13**, Heft 3-4, 601 (1970).

Jüntgen, H., "Review of the Kinetics of Pyrolysis and Hydropyrolysis in Relation to the Chemical Constitution of Coal," *Fuel*, **63**(6), 731 (1984).

Kahaner, D., C. Moler, and S. Nash, "Trigonometric Approximation and the Fast Fourier Transform," *Numerical Methods and Software*, Prentice-Hall, Englewood Cliffs, NJ (1989).

Kobayashi, H., J. B. Howard, and A. F. Sarofim, "Coal Devolatilization at High Temperature," *Int. Symp. on Combustion*, p. 411, Combustion Institute, Pittsburgh (1977).

Levenspiel, O., "Nonideal Flow," *Chemical Reaction Engineering*, 2nd ed., Wiley, New York (1972).

Little, J. N., and L. Shure, *Signal Processing Toolbox for Use with MatLab: User's Guide*, MathWorks, Inc., South Natick (1988).

Nilsson, T., "Modeling of Gasification in a Fluidized Bed," ScD Thesis, Kungl Tekniska Högskolan, Stockholm, CODEN: TRITA/KTR-90/29 (1990).

Press, W. H., B. P. Flannery, S. A. Teukolsky, and W. P. Vetterling, "Fourier Transform Spectral Methods," *Numerical Recipes*, Cambridge University Press (1986).

Pyle, D. L., and C. A. Zaror, "Heat Transfer and Kinetics in the Low Temperature Pyrolysis of Solids," *Chem. Eng. Sci.*, **39**(1), 147 (1984).

Seehra, M. S., and B. Ghosh, "Free Radicals, Kinetics and Phase Changes in the Pyrolysis of Eight American Coals," *J. Anal. Appl. Pyro.*, **13**, 209 (1988).

Solomon, P. R., D. G. Hamblen, R. M. Carangelo, and J. L. Krause, "Coal Thermal Decomposition in an Entrained Flow Reactor: Experiments and Theory," *Int. Symp. on Combustion*, p. 1139, Combustion Institute, Pittsburgh (1982).

Solomon, P. R., and D. G. Hamblen, "Finding Order in Pyrolysis Kinetics," *Prog. Energy Combust. Sci.*, **9**(4), 323 (1983).

Solomon, P. R., M. A. Serio, R. M. Carangelo, and J. R. Markham, "Very Rapid Coal Pyrolysis," *Fuel*, **65**(2), 182 (1986).

Suuberg, E. M., W. A. Peters, and L. B. Howard, "Coal Devolatilization," *Int. Symp. on Combustion*, p. 117, Combustion Institute, Pittsburgh (1978).

Appendix

```
% Loading of files A and C.
load Trial700

% Zero-time adjustment of file A.
maxA = find(A==max(A));
maxA = round(sum(maxA)/length(maxA));
q = 10*std(A(1:25));
for i = 26:maxA
  if A(i)>q, break, end
end
for j = maxA+1:length(A)
  if A(j)<q, break, end
end
A = A(i:j-1);

% Files A and C are normalized relative to tracer amount.
A = A - min(A); C = C - min(C);
C = C/sum(A); A = A/sum(A);
plot([C [A' NaN*(1:length(C)-length(A))]']), pause, % This
% is the figure 2 plot.

% File C is deconvolved, resulting in file B.
B = real(ifft(fft(C,8192)./fft(A,8192)));

% Power spectrum density analysis for determining the
% Butterworth filter design parameters. This part can be
omitted % once the parameters are found.
BB = fft(cumsum(B)); PBB = BB.*conj(BB)/4096;
t = 2*(0:2047)'/4096;
semilogy(t(1:50),PBB(1:50)), pause

% Iterative filtering of the cumulative sum of file B in a loop
% with 3 and 0.01 as Butterworth filter design parameters,
% followed by direct filtration.
B = flipud(B);
[a,b] = butter(3,.01);
for i = 1:10
  BB1 = cumsum(B);
  BB2 = filtfilt(a,b,BB1);
  B = diff((BB2+BB1)/2);
end
B = flipud(filtfilt(a,b,B));
B = B(1:4096);

% Correctness test of B, by convolving B with A and comparing
% the resulting file CC with the original C.
CC = real(ifft(fft(B,8192).*fft(A,8192)));
CC = CC(1:4096);
plot([B C CC]), % This is the figure 3 plot.
```

Manuscript received Apr. 5, 1991, and revision received July 15, 1991.